

Full length article

Fall risk assessment of active back-support exoskeleton-use for construction work using foot plantar pressure distribution

Akinwale Okunola ^a, Abiola Akanmu ^{a,*}, Houtan Jebelli ^b^a Myers-Lawson School of Construction, Virginia Tech, Blacksburg, VA, United States^b Department of Civil and Environmental Engineering, University of Illinois Urbana-Champaign, Urbana, IL, United States

ARTICLE INFO

Keywords:
 Exoskeleton
 Pressure Insole
 Fall risk
 Foot regions
 Foot plantar pressure
 Carpentry framing

ABSTRACT

In anticipation of the adoption of active back-support exoskeletons in the construction industry, the potential fall risks associated with these devices remain unclear. This study explores the unintended consequences stemming from exoskeleton usage, including the weight, bulkiness, and environmental factors that may contribute to fall risks. Specifically focusing on carpentry framing work, this study assesses the risk of falling while using an active back-support exoskeleton, employing foot plantar pressure distribution data captured with pressure insoles. A simulated framing task, comprising subtasks such as measuring, assembly, nailing, lifting, moving, and installation, was conducted both with and without the use of the active back-support exoskeleton. Foot plantar pressure distribution data for all foot regions were processed, and five pressure metrics were extracted for statistical analysis. Employing a combination of paired t-tests, ANOVA, and post-hoc tests, the findings reveal that the use of exoskeleton significantly increased the pressure metrics in at least one of the subtasks and foot regions, with an increase ranging from 7% to 51%. This suggests an elevated fall risk associated with using the device. Notably, the toe and heel regions are most sensitive to gait changes, while tasks involving movement, measuring, and assembly exhibit the highest fall risk. This study significantly contributes to the understanding of the previously unrecognized fall risk implications associated with active back support exoskeletons in the construction industry. The results explain the relationship between the foot region and construction tasks during exoskeleton-use. The results would inform construction stakeholders, facilitating informed decision-making regarding the adoption of active back support exoskeleton for construction tasks. Furthermore, the study provides valuable insights for the design of exoskeletons tailored to meet the unique demands of the construction work.

1. Introduction

In the effort to combat the occurrence of work-related musculoskeletal disorders (WMSDs) in the construction industry, exoskeletons have emerged as a potential solution. Exoskeletons aid in alleviating WMSDs by providing the necessary support to reduce the strain on the musculoskeletal systems [1,38]. Their potential has been demonstrated across various industries, particularly in the context of active and passive back-support exoskeletons, which have been shown to lessen WMSDs by reducing muscle activation (Antwi-Afari et al. 2021; [21,53] and range of motion [36]. For example, Walter et al. [53] examined the biomechanical advantage of an active back-support exoskeleton (aBSE) in weightlifting tasks. The study showed a decrease in muscle activation by 8 % to 22 % when using the exoskeleton. Huysamen et al. [21] evaluated the effectiveness of an aBSE in manual material handling tasks

by examining muscle activations, revealing reductions of 12 % to 15 % in muscle activity. Antwi-Afari et al. (2021) studied a passive back-support exoskeleton in repetitive lifting tasks within construction and found an 11 % minimum reduction in muscle activity in the back. Ogunseiju et al. [36] evaluated a postural-assist passive exoskeleton for manual material handling in construction and revealed a minimum reduction of 5 % in the range of motion during lifting task. However, there are unintended drawbacks associated with exoskeleton usage, such as discomfort in body parts [9], movement restrictions [39], thermal comfort [29], and catch and snag risks [25]. These issues can increase the mental workload of users, which could subsequently lead to reduced situational awareness, and thus indirectly increase the risk of fall [30]. Moreover, the weight of exoskeletons can shift the user's center of gravity [15,22,41], resulting in imbalance and an increased risk of fall. Active back-support exoskeletons are particularly

* Corresponding author.

E-mail address: abiola@vt.edu (A. Akanmu).

challenging due to their heavier weight compared to passive ones [18,51], which may exacerbate fall hazards in construction environments. According to the United States Bureau of Labor and Statistics (BLS 2020), fall-to-lower-level incidents occur at a rate of four times higher in the construction industry than in other industries. Falls in the construction industry have led to the disability of workers, and in severe cases, death [57].

Sensing technologies have been employed to assess fall risks and gait balancing across various industrial sectors. For example, Mehmood et al. [31] employed electromyography to capture and analyze lower leg muscles to evaluate fall risk in an elderly group. Haescher et al. (2018) utilized photoplethysmography data using a smart wearable wristwatch to assess and predict the risk of falling among older people. Annese and De Venuto [2] evaluated the risk of fall in a clinical environment by combining electroencephalogram sensor with other wearable sensors. Liu et al. [28] analyzed risk of falling among healthy and fall prone groups using inertia measurement unit. Nonetheless, research indicates that evaluating fall risk directly from foot plantar pressure measures exhibits a high sensitivity to changes in gait and balance [4,48]. Studies have assessed fall risks by assessing the foot plantar pressure distribution from force plates [33] and pressure insoles [4,55]. For example, Mickle et al. [33] assessed fall risk directly from all foot regions (i.e., heel, metatarsal, arch, and toe) using peak pressure and pressure-time integral metrics extracted from foot plantar pressure. Antwi-Afari and Li [4] utilized foot plantar pressure distribution measures, such as peak pressure, pressure-time integral, and average pressure, obtained from pressure insoles to evaluate the fall risk in construction. Yan et al. [55] used similar metrics from pressure insoles to evaluate fall risk among older people.

Despite the growing interest in the adoption of aBSE across various industry sectors, few studies have investigated fall risks when using the device for construction tasks. Considering the bulkiness and weight of aBSE, unintended consequences of using exoskeletons, and unstructured nature of construction sides, it is important to empirically evaluate the risk of falling while using aBSE for construction-related tasks. Therefore, this study aims to evaluate fall risks while using aBSE during carpentry framing work as a case study. This paper begins with an introduction of the study, followed by a background section to review relevant literature. The next section discusses the methods adopted for this study, followed by the results section. The last sessions include the discussion and conclusion sections. This study contributes by revealing the fall risks associated with using aBSE for construction work, offering insights into the impact of construction tasks and foot regions on fall risk during the use of aBSE.

2. Background

2.1. Potential fall hazards associated with exoskeleton usage

Exoskeletons have long been used in healthcare for rehabilitation and aiding mobility in individuals with physical challenges. More recently, they have been introduced in occupational settings to augment human musculoskeletal systems and reduce muscle strain. Exoskeletons provide support by supplying the torque to assist the body and can be categorized according to the body part they support, such as back, shoulder, or leg support [42]. They are also classified based on their source, either active (electrically powered) or passive (mechanically powered) [42].

Studies have shown that exoskeletons offer biomechanical benefits in reducing WMSDs by decreasing muscle strain (Antwi-Afari et al. 2021; [53], range of motion [43], and perceived discomfort [17]. For instance, Walter et al. [53] investigated the effect of aBSE during weight-lifting exercise and demonstrated a reduction of 5 % to 22 % in muscle activity. Poliero et al. [43] assessed the effect of using aBSE for performing tasks that include carrying and lifting of load and revealed a reduction of 10 % in the range of motion of the hip. Antwi-Afari et al. (2021)

investigated a passive back-support exoskeleton during repetitive lifting tasks in construction and observed a minimum reduction of 11 % in back muscle activity. Gonsalves et al. [17] examined the suitability of a passive back-support exoskeleton for rebar construction work and showed a reduction in perceived discomfort in the back region. Despite the reported benefits, unintended consequences of exoskeletons, which could indirectly or directly lead to fall hazards have been identified [40,50]. According to Zhu et al. [58], one of the major consequences of using exoskeletons is increase in cognitive load of users, which could indirectly increase their perception of fall risks as a result of reduced situational awareness. High cognitive load refers to the states at which the brain is trying hard to process the available information to meet the demand of a task, and excess of this demand could lead to mental fatigue [30]. In addition, the use of exoskeleton can restrict movement [37], cause thermal discomfort [29], and impact anthropometric fit [52], which could increase fall hazards. For example, Gonsalves et al. [17] assessed the use of exoskeletons in construction rebar tasks and identified increased pressure in the chest region due to exoskeleton use. Ogunseiju et al. [37] evaluated the suitability of exoskeletons in construction flooring work and revealed restriction in movement and interference with work during the use of the exoskeleton. Liu et al. [29] assessed the effect of thermal comfort on the use of exoskeletons in resting and lifting tasks across two different atmospheric temperatures, such as 26 and 10 degrees Celsius, representing hot and cold, respectively. The study revealed that the use of exoskeletons at high temperatures increases the metabolic rate, sweating, and thermal sensation, which leads to thermal discomfort for the users. Upasani et al. [52] assessed the potential of exoskeletons in agriculture tasks that involve lifting heavy loads, operating hand tools, and climbing. The study revealed that 30 % of the participants are concerned about fall risk due to the anthropometric fit of the exoskeleton.

Furthermore, researchers have unveiled some unintended consequences of using exoskeletons that could directly lead to fall hazards, such as the weight of the exoskeletons [15], uneven load distribution on the musculoskeletal system [41], and catch and snags [25]. For example, Fox et al. [15] conducted a comparative analysis of the potential of exoskeletons to improve manufacturing performances. Through reviews of existing studies, the study revealed the unintended consequences of added weight and misfit of exoskeletons which could lead to balancing problems, and as a result, an increase in fall risk. Picchiotti et al. [41] assessed the impact of exoskeleton on biomechanical loading of lumber spine in manual material handling tasks that involve lifting. The study revealed there is an unequal distribution of load across the body, which could also lead to imbalance of the body. Kim et al. [25] evaluated the potential of exoskeletons from the construction industry stakeholders' perspectives. Given the bulkiness of exoskeletons, one of the major concerns of the stakeholders is the catch and snag risks, which could lead to an increase in the risk of falling while working at height.

2.2. Assessment of fall risks

Sensing technologies have been employed to evaluate fall hazards across various sectors [8,12,14]. Examples of such sensing technologies include motion capture systems [10], electromyography (EMG) [27,31], photoplethysmography (PPG) (Haescher et al. 2018), electroencephalogram (EEG) [2], inertial measurement unit (IMU) [56], force plate [26], and pressure insoles [47]. However, researchers have shown that assessing fall risk directly from foot regions through metrics of foot plantar pressure displays high sensitivity to gait balancing changes [4]. Notable metrics, such as higher peak pressure, pressure-time integrals, pressure gradient, full width at half maximum, and average pressure, could disrupt balance and stability and lead to an increase in fall risk [33,55]. Force plates [23,32,33,35] and wearable pressure insole sensors [4,13]; Hapsari et al. 2014; [24,55] have been used to capture foot plantar pressure distributions for fall risk assessment. For instance, Mickle et al. [33] evaluated fall hazards among a group of older people,

classified into fallers and non-fallers, in a walking task. The foot plantar pressure distribution was captured for all foot regions using a force plate. The study shows that peak pressure and pressure-time integrals for the fallers are significantly higher than the non-fallers. Also, the heel, metatarsal, and toe regions of the foot show significantly higher peak pressure. Menz et al. [32] assessed the planter pressure distribution of callused and non-callused foot regions of elderly people while walking at selected speeds. The study computed the peak pressure across the foot regions and showed that people with calluses have a higher peak pressure, which shows they have balance impairments. Khalaf et al. [23] evaluated the plantar pressure alterations for balancing and stability in obese adults and a control group, which were classified according to the body mass index. The obese group shows higher peak pressure at the heel when compared to the control group, which indicates lesser postural stability that increases the risk of falling. Similarly, Neri et al. [35] investigated how the relationship between obesity and altered plantar pressure could lead to fall risk. The study compared obese, overweight, and normal weight groups while assessing the peak pressure of all the foot regions. The study shows that the obese group exerted the highest peak pressure in the midfoot and forefoot.

Given the ease of use and mobility advantage of wearable pressure insole sensors over a force plate, Yan et al. [55] evaluate fall hazards in older individuals classified into low-risk and high-risk falls, using pressure insoles for a walking task. The foot plantar pressure distribution was captured for all the foot regions. The study assessed the peak pressure, pressure-time integral, full width at half maximum, average pressure, and pressure gradient. The study showed that the pressure gradient has the best performance, with the heel and midfoot showing higher pressure. Foot plantar pressure distribution was captured using pressure insoles for all foot regions. Peak pressure, pressure-time integral, mean pressure, anterior/posterior center of pressure, and medial/lateral center of pressure were computed. The results showed significant differences across the loss of balance event compared to the control experiment. Kim et al. [24] compared the foot plantar pressure distributions of the dominant and non-dominant sides of participants with a history of falling. The peak plantar pressure was extracted and compared for the two sides. The peak pressure showed no statistical significance comparing the two sides. Hapsari et al. (2014) assessed the stability of high-heel wearers by evaluating the plantar pressure distributions of the foot regions while wearing different heights such as 0 cm, 4 cm, 7 cm, and 10 cm. The study showed that as the heel height increased, the peak pressure shifted from the rearfoot and midfoot regions to the forefoot and toe regions, which affected the stability of the users. Choi et al. [13] evaluated the difference in the fall risk for three slip events, normal step, recovered, and slipped using foot plantar pressure data captured for all the foot regions. The study assessed the peak pressure and pressure-time integral, which were compared for all three events. The study revealed that the heel is the most sensitive part of the foot for detecting fall risk. In construction, Antwi-Afari and Li [4] examined fall risk among construction workers, focusing on loss of balance events such as slips, trips, unexpected step-downs, and twisted ankles. The authors also used pressure insoles to measure foot plantar pressure distribution across all foot regions. And computed metrics including peak pressure, pressure-time integral, mean pressure, anterior/posterior center of pressure, and medial/lateral center of pressure. The results showed significant differences across the loss of balance events when compared to the control experiment.

3. Research gap

Existing research has identified risks associated with the use of aBSEs; however, a significant research gap exists as limited studies have explored the potential implications of these exoskeletons on fall risks during construction-related tasks. Construction activities involve dynamic motions and diverse postures, resulting in variable pressure levels across distinct foot regions. Studies have emphasized the critical role of

pressure distribution on foot regions as a key indicator of fall risk [4,32,33]. Despite the importance of understanding the impact of construction tasks on foot regions, a dearth of research exists in this domain. To address this research gap, it becomes imperative to explore the implications of aBSEs on fall risks during construction-related tasks. The intricate nature of construction tasks necessitates an investigation into how the use of these exoskeletons influences the risk of falls among users. Recognizing the multifaceted nature of construction tasks, it is crucial to unravel the contribution of different subtasks to the overall risk of falls when using aBSEs. This delineation is essential for developing targeted interventions and safety measures tailored to the specific challenges posed by various construction-related activities.

Moreover, pressure insoles present an opportunity to quantify a range of fall risk metrics or measures. These include peak plantar pressure, pressure-time integral, mean pressure, maximum pressure gradient, and full width at half maximum, allowing for an understanding of the impact on different foot regions. Thus, the study aims to fill the existing research gap and contribute valuable insights that can inform the design, implementation, and improvement of aBSEs for use in the construction industry. This study addresses the limited understanding of the influence of aBSEs on fall risks during construction-related tasks, exploring the relationship between exoskeleton use, construction sub-tasks, and foot region pressures. The overarching goal is to enhance safety protocols and design considerations in the construction industry by providing evidence-based insights into mitigating fall risks associated with the adoption of aBSEs.

4. Method

This section describes the approach employed to address the aforementioned gaps. These includes the participants involved in the study, the experimental design and procedure, the instruments utilized in the study, the data collected, and the data processing and analysis procedure. An overview of the methodology is illustrated in Fig. 1.

4.1. Participants

Sixteen healthy males (age: 30 ± 4 years, height: 173 ± 5.5 cm, body weight: 72 ± 7.5 kg, and body mass index: 23.98 ± 1.9 kg/m²) without any history of musculoskeletal disorders in the past six months were recruited for this study. Although some participants had previous exposure to construction tasks, their encounters were limited to laboratory settings, and they did not have regular construction framing task. Every participant gave their informed consent before commencing the experiment. The number of participants was selected based on a priori sample size computation, which provides a minimum power of 80 % with an effect size (f) and alpha (α) of 0.25 and 0.05, respectively. This yields a sample size of 8 participants, which is the minimum required for this study. All computations were performed using G*Power 3.1.9.7. This study was conducted in accordance with the approval of the Virginia Tech Institutional Regulatory Board (IRB: 19-796).

4.2. Experimental design and procedure

A carpentry framing task was repeatedly simulated under two experimental conditions, i.e., with-aBSE and without-aBSE. The framing task was carried out under six subtasks, such as measuring, assembly, nailing, lifting, moving, and installation, where foot planter pressure distributions were captured with wearable pressure insoles for four-foot regions (i.e., toe, metatarsal, arch, and heel) for the two legs. The independent factors are the experimental conditions, subtasks, and foot regions, while the dependent variables represent five metrics obtained from the foot plantar pressure. The five metrics are peak pressure, pressure-time integral, full width at half maximum, average pressure, and maximum pressure gradient. The duration of each experimental condition did not exceed five minutes to reduce the effect of fatigue and

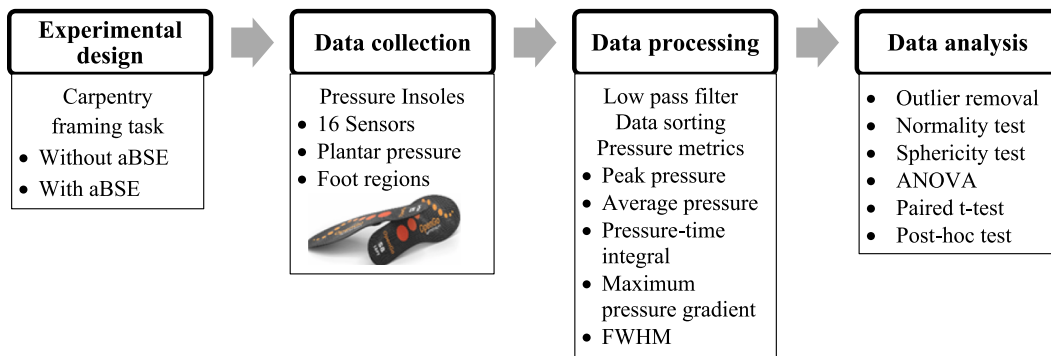


Fig. 1. Methodology overview.

the participants were allowed to rest for 30 min after completing the first experimental condition before proceeding to the second condition (Antwi-Afari et al. 2021). Prior to the commencement of the simulated framing task, each participant was educated about the nature of the task, and a step-by-step process of the experiment was demonstrated to the participants. Also, the participants were introduced to the operation modes of the aBSE and instructed on how the device would be used for the experiment. The experiment commenced with the measuring sub-task, where the participants measure out the required timber log out of the log of planks provided for the experiment. As shown in Fig. 2, the required timber logs for the frame construction consists of four numbers of $1.8\text{ m} \times 0.1\text{ m} \times 0.025\text{ m}$ and two numbers of $1.2\text{ m} \times 0.1\text{ m} \times 0.025\text{ m}$. This was followed by the assembly subtask, where the participants arranged the measured timber log to form the frame as indicated in Fig. 2. The next subtasks include fastening the assembled frame together with a nail gun. The fastened frame weighed approximately 20 kg, which is within the maximum safe lifting weight as provided by the revised National Institute for Occupational Safety and Health lifting equation [46,54]. The next subtask involves lifting the frame, which is subsequently moved manually to the upper floor via a staircase, where the final installation takes place. The experiment was recorded with a timestamp camera for ease of data sorting, according to the subtask, for analysis.

4.3. Instruments and data collection

4.3.1. Active back-support exoskeleton

Cray X active back-support exoskeleton, manufactured by German bionic company, was used for this study. The exoskeleton consists of

three major assistive strategies: lifting, bending, and walking, which can be regulated from 0 to 100 %. The device weighs approximately 7.5 kg. The exoskeleton is designed to be worn as a backpack with the help of straps shown in Fig. 3. The straps consist of chest, waist, shoulder, and thigh straps. The device is powered by a 40-Volt battery that could last 6 to 8 h according to the manufacturer.



Fig. 3. Active back-support exoskeleton. ce: .
Sour[16]

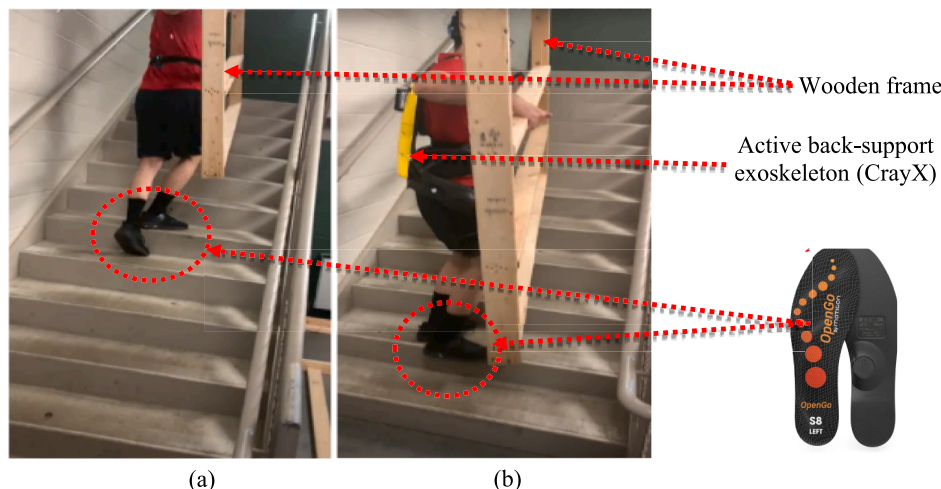


Fig. 2. Simulated carpentry task using pressure insole: (a) without aBSE and (b) with aBSE.

4.3.2. Pressure insoles

Opengo wearable pressure insoles manufactured by Moticon were adopted in this study to capture foot plantar pressure distribution across the foot regions for the two legs. Each insole consists of 16 sensors distributed across the foot regions. Sensors 1–4, 5–8, 9–13, and 14–16 capture the heel, the arch, the metatarsal, and the toe regions, respectively (Fig. 4) [11]. The pressure insole was adopted due to its capability to directly evaluate fall risk through gait changes as a result of exerted pressure distributed across the foot regions [33]. In this study, the metrics extracted from the foot plantar pressure distribution data across the foot regions to assess fall risk include peak plantar pressure, pressure-time integral, mean pressure, maximum pressure gradient, and full width at half maximum [4,55]. The peak plantar pressure represents the maximum pressure exerted by the participants on the ground at a particular point in time in each of the foot regions (Equation (1)). The peak pressure (PP) was computed for each of the six subtasks. The pressure-time integral (PTI) represents the total pressure exerted by the participants on the ground over the period of time covered while performing each of the subtasks (Equation (2)). The pressure-time integral was computed for each of the foot regions. The mean pressure (MP) is the average pressure exerted by participants on the ground over the duration of each subtask (Equation (3)). The average pressure was computed for all the foot regions. The maximum pressure gradient (MaxPG) represents the highest rate of change of the plantar pressure across the foot regions of the participants over the period of each of the subtasks (Equation (4)). The full width at half maximum (FWHM) represents the width of the pressure curve on the foot at half of its maximum height. The distance between the spots on the curve that corresponds to half of the peak pressure value is used to compute FWHM (Equation (5)). These metrics were computed using Eq. (1)–(5) below [4], Yan et al. [55].

$$PP = \text{Maximum} (P_i, \dots, P_N) \quad (1)$$

$$MP = \frac{1}{N} \sum_{i=0}^N P_i \quad (2)$$

$$PTI = \sum_{t=0}^N P_i X dt \quad (3)$$

$$MaxPG = \max_{t_1 \leq t \leq t_2} \frac{dP}{dt} \quad (4)$$

$$FWHM = t_2 - t_1 \quad (5)$$

Where P_i represents the pressure value at i -th sensor.

N represents the number of sensors.

dt represents the time interval.

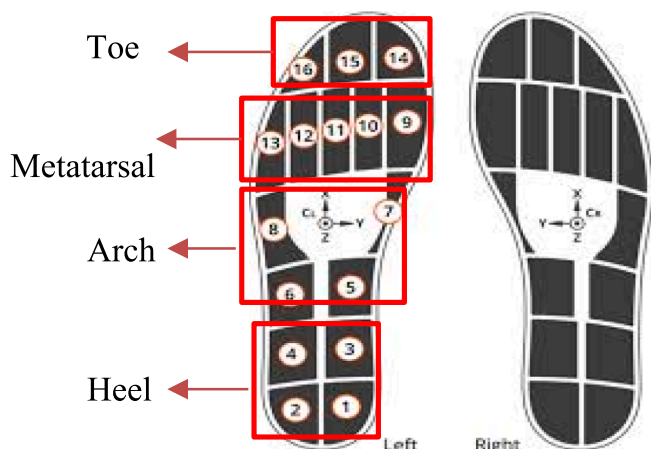


Fig. 4. Pressure insole sensors. .

Source: [34]

t_1 and t_2 are the start and end times of the contact phase.

4.3.3. Data processing and analysis

Data processing begins with the cleaning of the foot plantar pressure captured data from the pressure insoles during the experiment. According to Tandle et al. [49], physiological wearable sensors are susceptible to artifacts, which could significantly distort the quality of the results. While some of the artifacts could be intrinsic, i.e., generated via body movements, there are also extrinsic artifacts, generated by the electromagnetic devices within the vicinity [7]. Using the timestamp video recorded during the experiment and the timestamp on the foot plantar pressure distribution data, the data was sorted according to the subtasks (i.e., measuring, assembly, nailing, lifting, moving, and installation) to prepare it for filtering. The sorted data was passed through 12th-order Butterworth low-pass filtering with an 8 Hz cutoff frequency to remove the artifacts [44] as shown in Figs. 5a to 5f, which represents examples of a participant's data. The next step was to compute the fall risk metrics (i.e., peak pressure, pressure-time integral, full width at half maximum, average pressure, and maximum pressure gradient) using Equations 1 to 6 in accordance with each of the subtasks.

Regarding the statistical analysis, firstly, Tukey's range test was used to remove the outliers using the interquartile range to define the lower limit ($Q1 - 1.5 * IQR$) and upper limit ($Q3 + 1.5 * IQR$) [45]. Given the repeated nature of the experiment, the sphericity and normality assumptions of the data were examined using Mauchly and Shapiro-Wilk tests to determine the suitability of the statistical tools to be deployed to examine the significant differences. Having met the required assumptions, a 3-way repeated measures ANOVA was conducted to examine the statistical differences among the variables. Paired *t*-test was further conducted to examine the differences in each of the foot regions across all of the subtasks. Also, 1-way repeated measure ANOVA was adopted to understand the significant subtask and the foot region while using aBSE. The independent variables are the experimental conditions (without-aBSE and with-aBSE), the foot regions (toe, heel, metatarsal, and arch), and the subtasks, while the dependent variables are peak pressure, pressure-time integral, full width at half maximum, average pressure, and maximum pressure gradient. All results were presented using bar graphs and tables showing the statistical significance. Eta Squared (η^2) and Cohen's *d* were reported to estimate the effect sizes for the ANOVA and paired *t*-test, respectively. MATLAB 2023Ra has been adopted for the processing of data, while Microsoft Excel and JMP Pro 17.0.0. have been employed in conducting statistical analysis.

5. Results

This section illustrates the results of the fall risk assessments for the experimental conditions in this study. The normality test results for both the Exo and Nexo conditions are shown in Tables 1 and 2, respectively. Table 3 indicates Greenhouse Geisser corrections ($p < 0.05$) for the sphericity of the datasets. Figs. 6–10 present the results of the analysis according to the following metrics: peak pressure, mean pressure, pressure-time integral, maximum pressure gradient, full width at half maximum, and minimum pressure gradient. 'Nexo' and 'Exo' are the results of these metrics for the without-aBSE and with-aBSE conditions respectively.

5.1. Peak pressure

Fig. 6 illustrates the results of the fall risk evaluation through the lens of the peak pressure. The 3-way repeated measure shows that the experimental conditions (without-aBSE and with-aBSE) are significant ($F = 23.69, P = <0.00, \eta^2 = 0.012$), with a higher peak pressure observed while using the aBSE. A paired *t*-test further revealed the differences in the foot regions (heel, arch, metatarsal, and toe) by comparing the peak pressure of the two experimental conditions for each of the subtasks. In measuring subtask, all the peak pressures for the

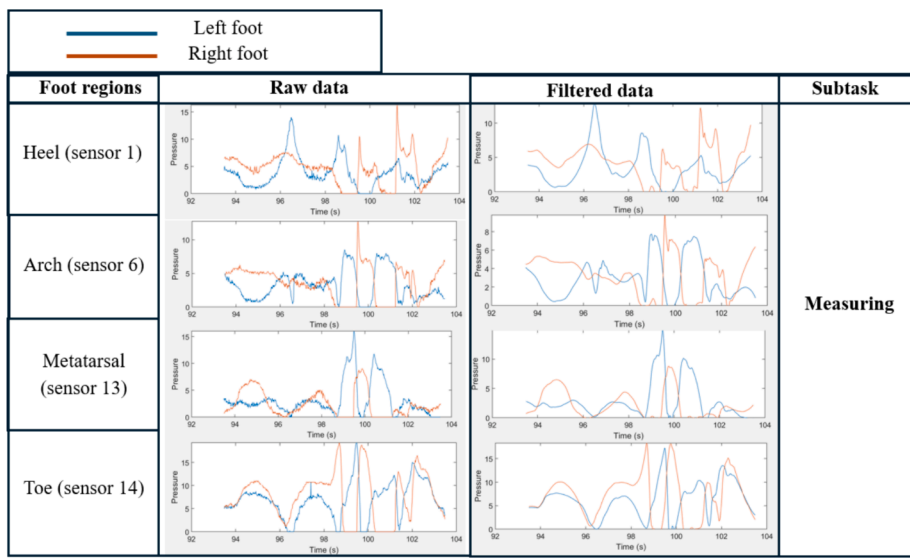


Fig. 5a. Example of data processing for participant 1 across all foot regions for measuring subtask.

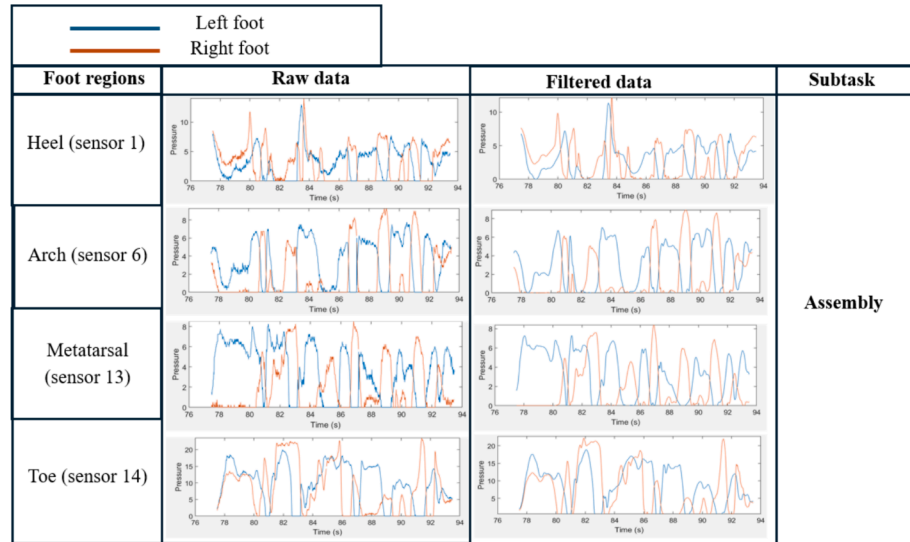


Fig. 5b. Example of data processing for participant 1 across all foot regions for assembly subtask.

foot regions are significantly ($p < 0.05$) higher while using the aBSE, such that the heel ($t(15) = 3.22, P = 0.00, d = 0.81$), arch ($t(15) = 3.94, P = 0.00, d = 0.99$), metatarsal ($t(15) = 2.99, P = 0.00, d = 0.75$), and toe ($t(15) = 2.74, P = 0.00, d = 0.69$) increased by 12.4 %, 15.6 %, 22.6 %, and 12.1 %, respectively. In the assembly subtask, only the arch region has a significant ($t(15) = 1.80, P = 0.04, d = 0.45$) higher peak pressure of 7.4 % in the with-aBSE condition. While performing the nailing subtask, the peak pressure was significantly ($p < 0.05$) higher in the regions of arch ($t(15) = 3.65, P = 0.00, d = 0.91$), metatarsal ($t(15) = 2.56, P = 0.01, d = 0.64$), and toe ($t(15) = 1.89, P = 0.04, d = 0.47$), with percentage increases of 11.4 %, 17.3 %, and 9.7 %, respectively. Only the heel region shows a significant ($p < 0.05$) increase in with-aBSE condition while performing lifting ($t(15) = 3.09, P = 0.00, d = 0.77$) and moving ($t(15) = 4.54, P = 0.00, d = 1.14$) subtasks with percentages of 11.4 % and 14.2 %, respectively. In the installing subtask, the arch ($t(15) = 2.34, P = 0.02, d = 0.59$), metatarsal ($t(15) = 3.76, P = 0.00, d = 0.94$), and toe ($t(15) = 2.06, P = 0.00, d = 0.69$) have a significantly higher peak pressure of 18.8 %, 38.7 %, and 20.8 %, respectively, while using the aBSE. Significantly ($p < 0.05$), in the with-aBSE condition, the heel and toe are the foot regions with the highest peak pressure for

moving ($F = 40.05, P = <0.00, \eta^2 = 0.68$) and measuring ($F = 28.42, P = <0.00, \eta^2 = 0.58$), subtasks, while the heel was solely the highest for the remaining subtasks such as assembly ($F = 54.86, P = <0.00, \eta^2 = 0.60$), nailing ($F = 19.70, P = <0.00, \eta^2 = 0.52$), lifting ($F = 35.26, P = <0.00, \eta^2 = 0.61$), and installation ($F = 15.95, P = <0.00, \eta^2 = 0.30$). Comparing the peak pressure of all the subtasks while using the abSE, the participants significantly ($F = 3.84, P = 0.00, \eta^2 = 0.053$) experienced higher peak pressure during the moving subtask.

For the interaction effects, the experimental conditions and the foot regions show no statistical significance ($F = 0.54, P = 0.65, \eta^2 = 0.000$). While the experimental conditions and subtasks show statistical significance ($F = 2.35, P = <0.04, \eta^2 = 0.005$) for the interaction effect, the post-hoc test revealed a moving subtask, and the with-aBSE experimental condition shows the highest peak pressure. Similarly, the interaction effect for the foot regions and subtasks shows statistical significance ($F = 1.84, P = 0.03, \eta^2 = 0.014$), with the post-hoc test revealing the heel region and assembly subtask having the highest peak pressure. The last interaction effect, which consists of the experimental conditions, foot regions, and subtasks, shows no statistical significance ($F = 0.74, P = 0.75, \eta^2 = 0.056$).

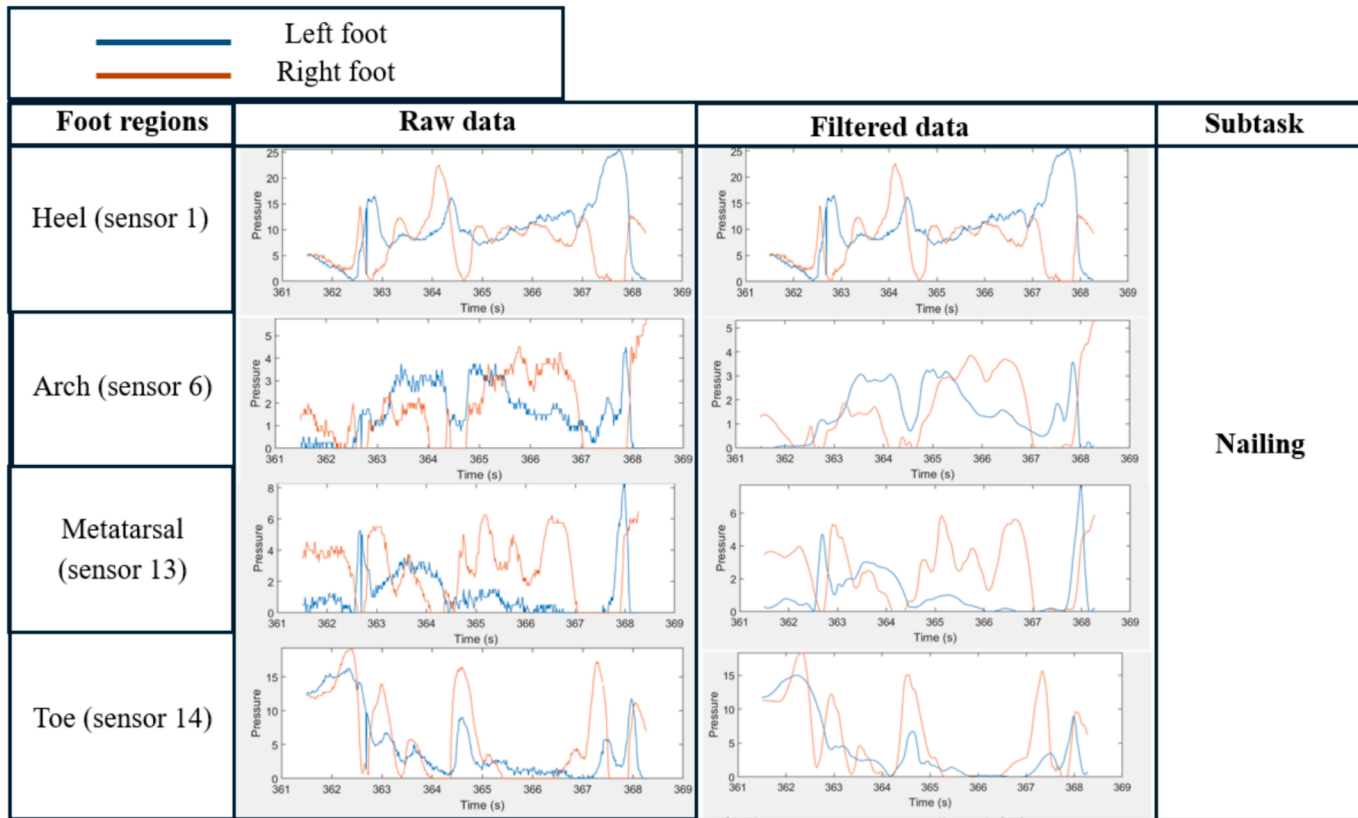


Fig. 5c. Example of data processing for participant 1 across all foot regions for nailing subtask.

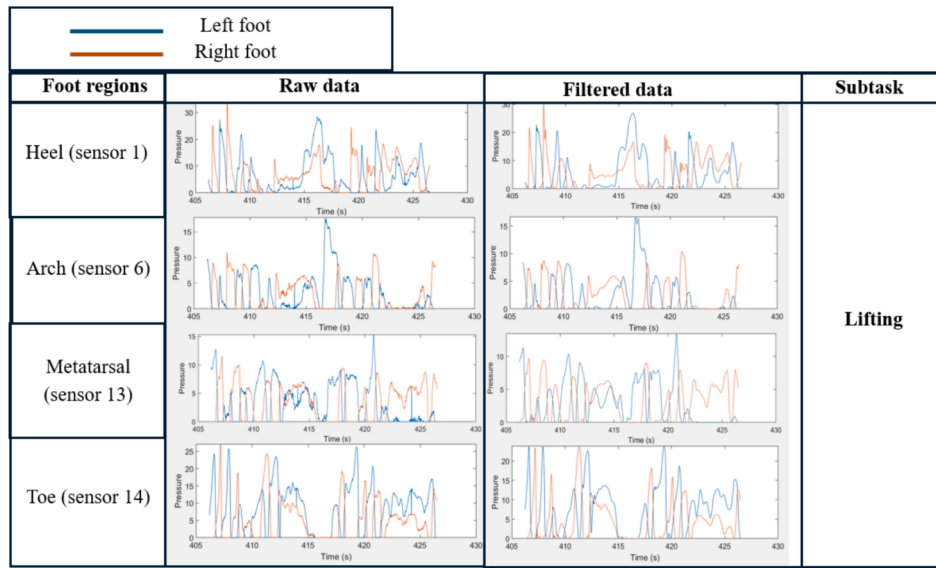


Fig. 5d. Example of data processing for participant 1 across all foot regions for lifting subtask.

5.2. Mean pressure

Fig. 6 denotes the outcomes of the evaluations of fall risk from the perspective of average pressure. Examining the experimental conditions' main effect, there is no statistical difference ($F = 0.55, P = 0.46, \eta^2 = 0.006$). However, a paired *t*-test further examines the differences in the mean pressure for each of the foot regions in each of the subtasks. For instance, there is no statistical difference ($p > 0.05$) in all the four-foot regions, i.e., heel ($t(15) = 0.41, P = 0.34$), arch ($t(15) = 1.41, P = 0.08$,

metatarsal ($t(15) = 1.36, P = 0.09$), and toe ($t(15) = 1.349, P = 0.10$) while performing the measuring subtask. While performing the assembly task, only the toe region has a statistical difference ($t(15) = 1.93, P = 0.04, d = 0.48$) while using the aBSE with an increase of 14.2 %. In the nailing subtask, the arch ($t(15) = 4.11, P = 0.00, d = 1.03$) and metatarsal ($t(15) = 2.06, P = 0.03, d = 0.52$) regions have a significant ($p < 0.05$) higher mean pressure of 19.4 % and 17.1 %, respectively, while using the aBSE. For the lifting subtask, only the metatarsal has a significant ($t(15) = 2.70, P = 0.00, d = 0.68$) increment of 27.6 % in the

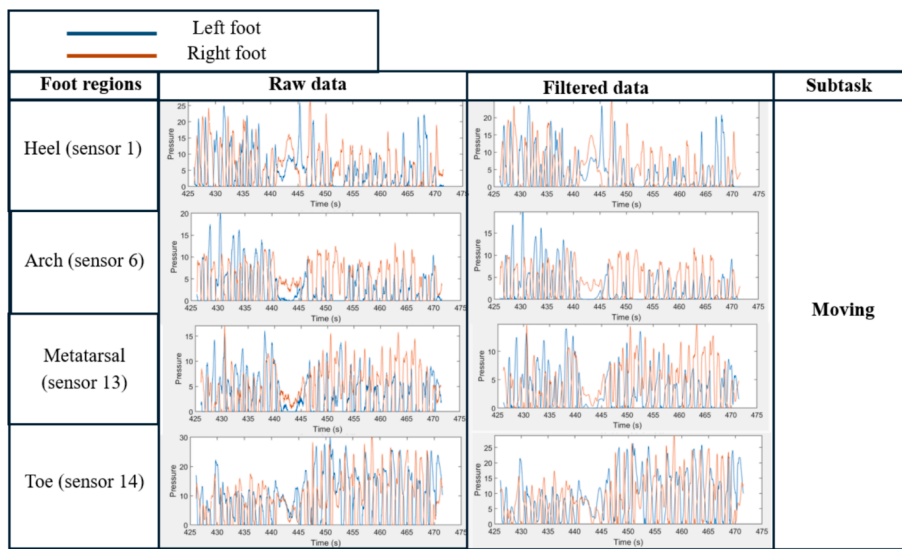


Fig. 5e. Example of data processing for participant 1 across all foot regions for moving subtask.

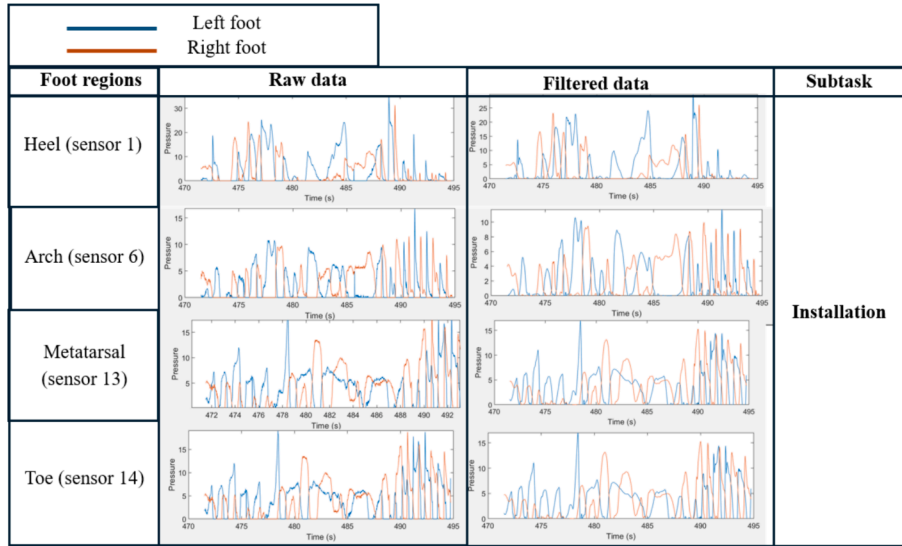


Fig. 5f. Example of data processing for participant 1 across all foot regions for installation subtask.

with-aBSE condition. A significant increase ($t(15) = 4.14, P = 0.00, d = 1.04$) of 16 % was experienced in the arch region while using the aBSE in the moving subtask. While performing the installation subtask, the use of aBSE significantly ($p < 0.05$) increases the metatarsal ($t(15) = 4.03, P = 0.00, d = 1.01$) and toe ($t(15) = 2.53, P = 0.01, d = 0.63$) regions by 49 % and 20.4 %, respectively. Comparing the foot regions of each subtask while using the aBSE, the toe significantly ($p > 0.05$) has the highest mean pressure while performing assembly ($F = 21.59, P = <0.00, \eta^2 = 0.43$), nailing ($F = 8.21, P = <0.00, \eta^2 = 0.25$), lifting ($F = 8.17, P = <0.00, \eta^2 = 0.28$), and installation ($F = 3.03, P = <0.00, \eta^2 = 0.14$) subtasks. The toe and heel have the highest ($p > 0.05$) mean pressure for measuring ($F = 15.55, P = <0.00, \eta^2 = 0.37$) subtask, while moving ($F = 2.63, P = 0.07, \eta^2 = 0.11$) subtask show no significance ($p < 0.05$). While using the aBSE, comparison of the mean pressure of all the subtasks shows no statistical significance ($F = 0.63, P = 0.67, \eta^2 = 0.06$).

Regarding the interaction effects, the experimental conditions and foot regions show no statistical significance ($F = 0.27, P = 0.84, \eta^2 = 0.000$). Similarly, the interaction effect of the experimental conditions and subtasks shows no statistical significance ($F = 0.18, P = 0.97, \eta^2 = 0.06$).

0.000). In contrast, the interaction effects of the foot regions and subtasks indicate statistical significance ($F = 2.88, P = <0.00, \eta^2 = 0.028$), with the post-hoc test indicating the toe region and assembly subtask having the highest average pressure. Lastly, there is no significance ($F = 0.68, P = 0.80, \eta^2 = 0.006$) in the interaction effects of the experimental conditions, foot regions, and subtasks.

5.3. Pressure-Time integral

Fig. 7 illustrates the results of the pressure-time integral for the evaluation of fall risk in this study. The experimental condition's main effect shows no statistical difference ($F = 0.98, P = 0.33, \eta^2 = 0.003$). However, the paired t -test results show significance in some instances when comparing the pressure-time integral for each foot region for all the subtasks. For instance, in the measuring, assembly, and nailing subtasks, none of the foot regions is significant in both experimental conditions for the three subtasks. In lifting subtask, only the metatarsal foot region has a significant ($t(15) = 3.04, P = 0.00, d = 0.76$) increase of 51 % while using the aBSE. In moving subtask, all four foot regions are significantly higher when using the aBSE by 50.2 %, 50.2 %, 37.7 %, and

Table 1

Shapiro-Wilk test results for Exo condition (p-value > 0.05 indicates normality).

Metrics	Foot regions	Measuring P-value(W-stat)	Assembly P-value(W-stat)	Nailing P-value(W-stat)	Lifting P-value(W-stat)	Moving P-value(W-stat)	Installation P-value(W-stat)
Peak pressure	Heel	0.30(0.87)	0.23(0.92)	0.60(0.95)	0.62(0.95)	0.95(0.98)	0.82(0.96)
	Arch	0.53(0.95)	0.07(0.88)	0.88(0.96)	0.99(0.98)	0.62(0.95)	0.46(0.94)
	Metatarsal	0.72(0.96)	0.31(0.95)	0.18(0.91)	0.37(0.93)	0.46(0.94)	0.11(0.89)
	Toe	0.06(0.86)	0.19(0.91)	0.72(0.96)	0.12(0.89)	0.75(0.96)	0.34(0.92)
Pressure-time integral	Heel	0.69(0.96)	0.79(0.96)	0.22(0.92)	0.99(0.99)	0.44(0.94)	0.65(0.96)
	Arch	0.99(0.99)	0.44(0.94)	0.13(0.91)	0.60(0.95)	0.25(0.93)	0.79(0.96)
	Metatarsal	0.07(0.88)	0.22(0.93)	0.35(0.93)	0.88(0.97)	0.27(0.93)	0.25(0.92)
	Toe	0.82(0.97)	0.33(0.94)	0.65(0.96)	0.62(0.96)	0.26(0.92)	0.21(0.92)
Max PG	Heel	0.96(0.98)	0.29(0.93)	0.82(0.97)	0.75(0.96)	0.12(0.91)	0.83(0.97)
	Arch	0.62(0.95)	0.48(0.87)	0.97(0.98)	0.12(0.89)	0.18(0.88)	0.63(0.95)
	Metatarsal	0.93(0.97)	0.56(0.95)	0.22(0.92)	0.40(0.88)	0.33(0.94)	0.18(0.92)
	Toe	0.8(0.97)	0.64(0.92)	0.12(0.91)	0.30(0.88)	0.95(0.97)	0.45(0.94)
Average pressure	Heel	0.69(0.96)	0.93(0.97)	0.24(0.93)	0.15(0.91)	0.12(0.91)	0.84(0.97)
	Arch	0.95(0.98)	0.99(0.98)	0.42(0.94)	0.09(0.89)	0.06(0.87)	0.07(0.89)
	Metatarsal	0.33(0.93)	0.42(0.94)	0.22(0.92)	0.26(0.93)	0.47(0.94)	0.56(0.95)
	Toe	0.44(0.94)	0.79(0.97)	0.12(0.90)	0.28(0.93)	0.43(0.94)	0.1(0.90)
FHW	Heel	0.89(0.97)	0.05(0.88)	0.41(0.94)	0.19(0.92)	0.08(0.89)	0.97(0.98)
	Arch	0.68(0.96)	0.13(0.90)	0.13(0.91)	0.23(0.92)	0.16(0.92)	0.87(0.97)
	Metatarsal	0.95(0.98)	0.29(0.93)	0.13(0.91)	0.24(0.93)	0.06(0.89)	0.59(0.95)
	Toe	0.82(0.97)	0.13(0.89)	0.46(0.94)	0.18(0.92)	0.13(0.91)	0.72(0.96)

Table 2

Shapiro-Wilk test results for Nexo condition (p-value > 0.05 indicates normality).

Metrics	Foot regions	Measuring P-value(W-stat)	Assembly P-value(W-stat)	Nailing P-value(W-stat)	Lifting P-value(W-stat)	Moving P-value(W-stat)	Installation P-value(W-stat)
Peak pressure	Heel	0.29(0.93)	0.41(0.94)	0.25(0.92)	0.64(0.96)	0.66(0.96)	0.48(0.94)
	Arch	0.19(0.29)	0.21(0.92)	0.29(0.93)	0.68(0.96)	0.98(0.98)	0.09(0.89)
	Metatarsal	0.99(0.99)	0.73(0.96)	0.77(0.96)	0.41(0.94)	0.41(0.94)	0.29(0.92)
	Toe	0.37(0.94)	0.33(0.94)	0.24(0.93)	0.13(0.90)	0.35(0.93)	0.67(0.95)
Pressure-time integral	Heel	0.99(0.98)	0.73(0.96)	0.91(0.97)	0.76(0.97)	0.21(0.93)	0.26(0.93)
	Arch	0.46(0.95)	0.77(0.96)	0.30(0.93)	0.76(0.95)	0.70(0.96)	0.22(0.93)
	Metatarsal	0.11(0.91)	0.40(0.94)	0.97(0.98)	0.48(0.95)	0.16(0.91)	0.14(0.89)
	Toe	0.10(0.91)	0.60(0.96)	0.13(0.91)	0.54(0.95)	0.62(0.96)	0.17(0.92)
MaxPG	Heel	0.88(0.97)	0.80(0.97)	0.12(0.91)	0.97(0.79)	0.84(0.97)	0.79(0.97)
	Arch	0.41(0.94)	0.55(0.95)	0.83(0.97)	0.97(0.82)	0.07(0.89)	0.13(0.88)
	Metatarsal	0.44(0.94)	0.10(0.90)	0.09(0.89)	0.09(0.90)	0.07(0.90)	0.29(0.93)
	Toe	0.98(0.98)	0.86(0.97)	0.16(0.92)	0.61(0.95)	0.45(0.94)	0.06(0.89)
Average pressure	Heel	0.92(0.97)	0.83(0.97)	0.32(0.94)	0.53(0.95)	0.64(0.96)	0.14(0.91)
	Arch	0.89(0.97)	0.63(0.96)	0.99(0.99)	0.20(0.92)	0.76(0.96)	0.31(0.94)
	Metatarsal	0.80(0.97)	0.87(0.97)	0.60(0.96)	0.45(0.95)	0.42(0.95)	0.94(0.98)
	Toe	0.16(0.92)	0.27(0.93)	0.38(0.94)	0.19(0.92)	0.61(0.96)	0.52(0.95)
FHW	Heel	0.67(0.96)	0.31(0.89)	0.25(0.92)	0.14(0.91)	0.11(0.91)	0.24(0.92)
	Arch	0.72(0.96)	0.31(0.89)	0.40(0.93)	0.10(0.90)	0.08(0.89)	0.21(0.91)
	Metatarsal	0.66(0.97)	0.06(0.88)	0.16(0.89)	0.05(0.88)	0.15(0.92)	0.09(0.89)
	Toe	0.89(0.97)	0.05(0.88)	0.05(0.88)	0.11(0.90)	0.88(0.97)	0.06(0.88)

Table 3

Greenhouse-Geisser sphericity corrections (p-value < 0.05 indicates significance).

Metrics	Greenhouse-Geisser	Df	Mean Square	F	Significance
Peak pressure	0.59	4.13	1213.57	140.38	<0.001
Pressure-time integral	0.42	2.93	319709.51	17.71	<0.001
MaxPG	0.49	3.44	417.85	84.12	<0.001
Mean pressure	0.42	2.94	113.29	61.88	<0.001
FHW	0.19	1.33	4,593,125,677	22.31	<0.001

27.1 % for the heel ($t(15) = 2.41, P = 0.02, d = 0.61$), arch ($t(15) = 2.74, P = 0.00, d = 0.69$), metatarsal ($t(15) = 3.23, P = 0.00, d = 0.81$), and toe ($t(15) = 2.51, P = 0.01, d = 0.63$) regions, respectively. While performing the installation subtask with abSE, only the metatarsal ($t(15) = 2.97, P = 0.00, d = 0.74$ and toe ($t(15) = 2.34, P = 0.02, d =$

0.59) regions are significantly higher by 45.4 % and 46 %, respectively. The pressure-time integral was compared for all the subtasks; assembly and measuring subtasks had the highest significant ($F = 64.62, P = <0.00, \eta^2 = 0.44$) value. While using the abSE, the toe foot region significantly ($p < 0.05$) has the highest pressure-time integral across all the subtasks i.e., measuring ($F = 10.71, P = <0.00, \eta^2 = 0.26$), assembly ($F = 19.30, P = <0.00, \eta^2 = 0.25$), nailing ($F = 5.43, P = <0.00, \eta^2 = 0.18$), lifting ($F = 28.42, P = <0.00, \eta^2 = 0.16$), moving ($F = 10.37, P = <0.00, \eta^2 = 0.04$), and installation ($F = 3.69, P = 0.02, \eta^2 = 0.09$).

Regarding the interaction effect, experimental conditions and foot regions display no significant ($F = 0.05, P = 0.98, \eta^2 = 0.000$) interaction effects. Similarly, the experimental conditions and subtasks show no statistical difference ($F = 1.27, P = 0.27, \eta^2 = 0.003$) as well. However, there is a significant ($F = 9.63, P = <0.00, \eta^2 = 0.071$) interaction effect between the foot regions and subtasks, with the post-hoc test revealing the 'toe region and assembly subtask' and 'toe region and measuring subtask' having the highest pressure-time integral value. Lastly, there is no statistical difference ($F = 0.26, P = 0.99, \eta^2 = 0.002$) in the interaction effect of the experimental conditions, foot regions, and subtasks.

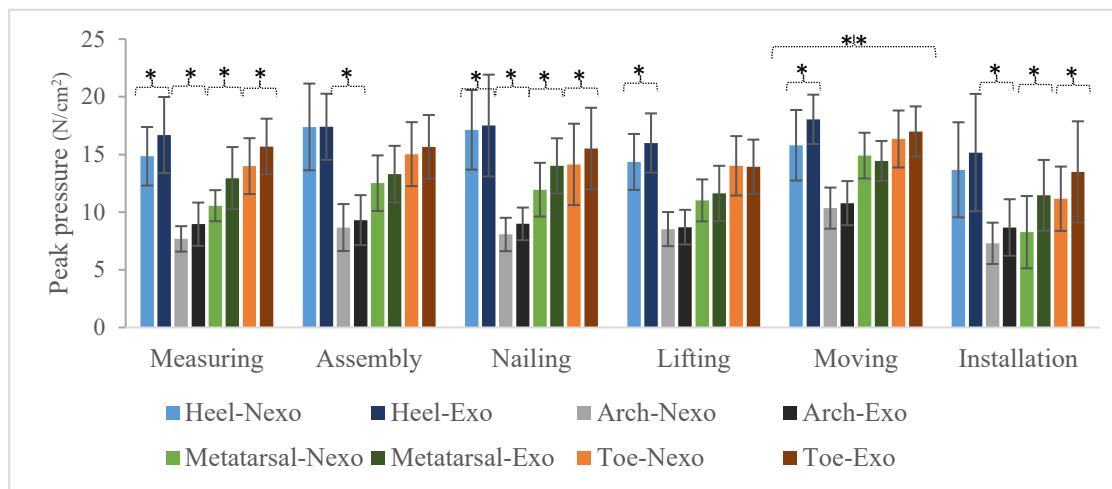


Fig. 6. Peak pressure at foot regions during carpentry framing tasks. ("*" and "****" = significant at p-value < 0.05).

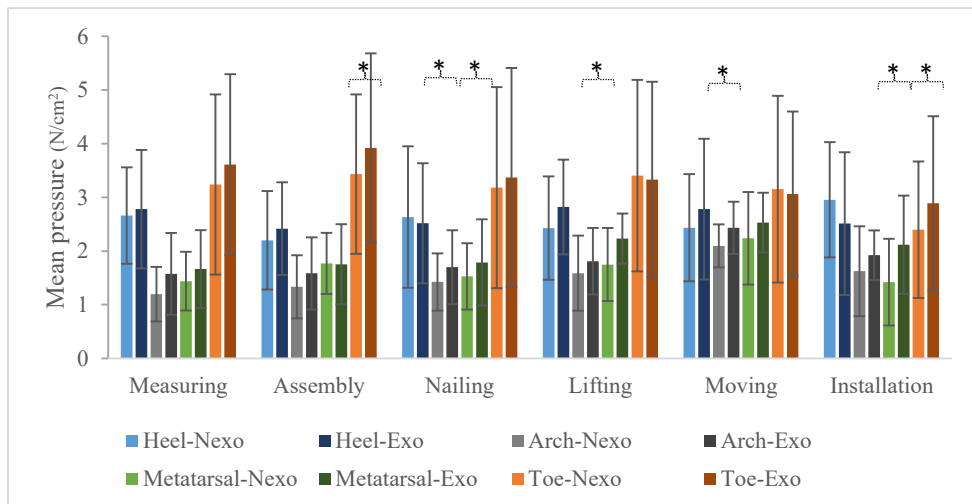


Fig. 7. Mean pressure at foot regions during carpentry framing tasks. ("*" = significant at p-value < 0.05).

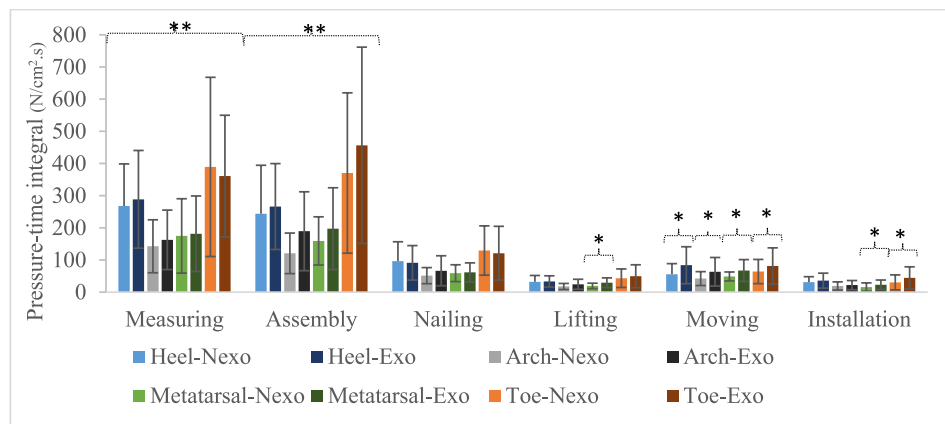


Fig. 8. Pressure-time integral at foot regions during carpentry framing tasks. ("*" and "****" = significant at p-value < 0.05).

5.4. Maximum pressure gradient (Max PG)

Fig. 8 depicts the results of the maximum pressure gradient metric for evaluating fall risk. For the main effect of the experimental conditions, there is no statistical significance ($F = 0.02, P = 0.88, \eta^2 = 0.000$).

The use of a paired *t*-test to examine the difference in the maximum pressure gradient for each foot region for all the subtasks, however, revealed some statistical differences. For instance, in the measuring subtask, the use of the abSE significantly ($t(15) = -2.07, P = 0.03, d = -0.52$) increases the arch foot region by 9.9 %. In contrast, the without-

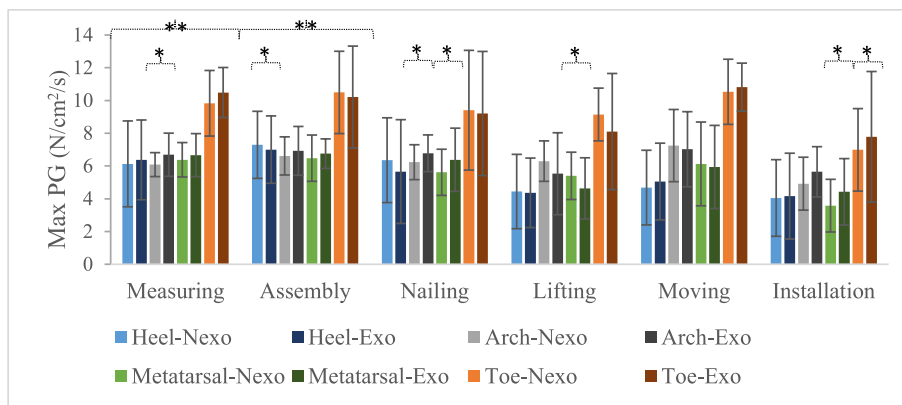


Fig. 9. Maximum pressure gradient at foot regions during carpentry framing tasks. (“*” and “**” = significant at p -value < 0.05).

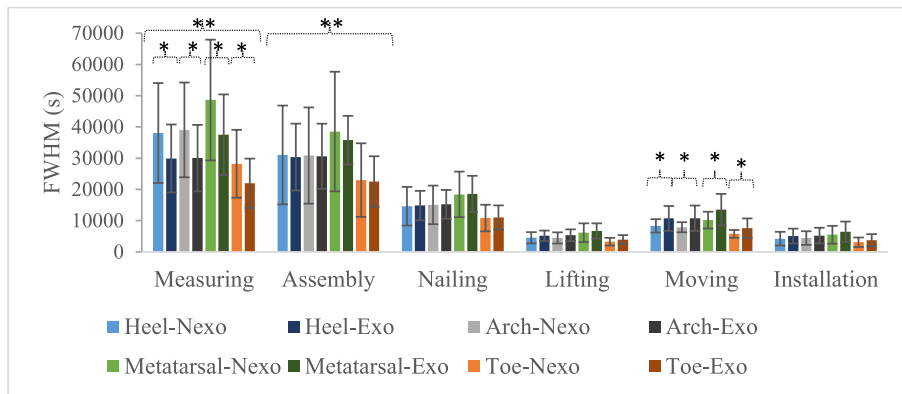


Fig. 10. Full width at half maximum at foot regions during carpentry framing tasks. (“*” and “**” = significant at p -value < 0.05).

abSE condition shows a higher significant ($t(15) = -2.62, P = 0.01, d = -0.66$) difference of 4.2 % in the heel while performing assembly subtask. In nailing subtask, the use of abSE shows a significant ($p < 0.05$) increase of 8.7 % and 13.6 % in the regions of the arch ($t(15) = 2.92, P = 0.00, d = 0.73$) and metatarsal ($t(15) = 2.28, P = 0.02, d = 0.57$), respectively. While using the abSE in lifting subtask, the metatarsal region of the foot shows a significant ($t(15) = -2.07, P = 0.03, d = -0.52$) increase of 16.5 %. Moving subtask show no statistical significance, but the installation subtask revealed higher peak pressure at the metatarsal ($t(15) = 2.77, P = 0.00, d = 0.69$) and toe ($t(15) = 3.15, P = 0.00, d = 0.79$). While using the abSE, comparing the maximum pressure gradient of all the subtasks shows that assembly and measuring subtasks have the highest ($F = 7.58, P = <0.00, \eta^2 = 0.07$) value. For all the subtasks, similar to the pressure-time integral, the toe foot region has the highest significant ($p < 0.05$) maximum pressure gradient i.e., measuring ($F = 20.67, P = <0.00, \eta^2 = 0.47$), assembly ($F = 10.78, P = <0.00, \eta^2 = 0.46$), nailing ($F = 10.72, P = <0.00, \eta^2 = 0.25$), lifting ($F = 19.19, P = <0.00, \eta^2 = 0.26$), moving ($F = 32.99, P = <0.00, \eta^2 = 0.36$), and installation ($F = 13.92, P = 0.02, \eta^2 = 0.24$).

Regarding the interaction effects, the experimental conditions and foot regions show no statistical significance ($F = 0.18, P = 0.90, \eta^2 = 0.000$). Similarly, the experimental conditions and subtask interaction effect show no statistical significance ($F = 1.32, P = 0.25, \eta^2 = 0.003$). However, the foot regions and subtasks interaction effect show statistical significance ($F = 2.13, P = 0.00, \eta^2 = 0.016$), with the post-hoc test revealing the ‘toe region and assembly subtask’ and ‘toe region and moving subtask’ having the highest maximum pressure gradient value. The last interaction effect of experimental conditions, foot regions, and subtasks shows no statistical significance.

5.5. Full width at half maximum (FWHM)

The results of the full width at half maximum assessment of the fall risk of using abSE for framing task are revealed in Fig. 8. The experimental conditions’ main effect shows no statistical significance ($F = 0.28, P = 0.60, \eta^2 = 0.000$). The paired t -test comparing the FWHM of each foot region of all the subtasks, however, shows some significance. For example, measuring subtask for the without-abSE condition shows that all the foot regions are significantly ($p < 0.05$) higher by 27.2 %, 30.1 %, 29.6 %, and 28.5 % for the regions of heel ($t(15) = -1.79, P = 0.04, d = -0.45$), arch ($t(15) = -2.11, P = 0.03, d = -0.53$), metatarsal ($t(15) = -1.96, P = 0.04, d = -0.49$), and toe ($t(15) = -1.92, P = 0.04, d = -0.48$), respectively. In contrast, in the moving subtask of the with-abSE condition, all the foot regions i.e., heel ($t(15) = 2.87, P = 0.00, d = 0.72$), arch ($t(15) = 2.78, P = 0.00, d = 0.70$), metatarsal ($t(15) = 3.35, P = 0.00, d = 0.84$), and toe ($t(15) = 2.29, P = 0.02, d = 0.57$) are statistically ($p < 0.05$) higher by 28.4 %, 36.5 %, 32.6 %, and 31.6 %, respectively. There is no statistical significance in the remaining subtasks (assembly, nailing, lifting, and installation). Comparing all the subtasks while using abSE shows that measuring and assembly subtasks show the highest ($F = 166.17, P = <0.00, \eta^2 = 0.68$) FWHM. For all the subtasks, the metatarsal foot region has the highest significant ($p < 0.05$) maximum pressure gradient i.e., measuring ($F = 111.61, P = <0.00, \eta^2 = 0.22$), assembly ($F = 204.46, P = <0.00, \eta^2 = 0.27$), nailing ($F = 114.59, P = <0.00, \eta^2 = 0.25$), lifting ($F = 75.70, P = <0.00, \eta^2 = 0.22$), moving ($F = 101.44, P = <0.00, \eta^2 = 0.22$), and installation ($F = 44.02, P = <0.00, \eta^2 = 0.13$).

Regarding the interaction effects, the experimental conditions and foot regions show no statistical difference ($F = 0.15, P = 0.93, \eta^2 = 0.000$). However, the interaction effect of experimental conditions and subtasks shows statistical difference ($F = 9.37, P = <0.00, \eta^2 = 0.015$)

with the with-aBSE condition and measuring subtask having the highest value of FWHM. Similarly, the interaction effect of the foot regions and subtasks indicates a statistical significance ($F = 3.95, P = <0.00, \eta^2 = 0.019$), with the metatarsal foot region and measuring subtask showing the highest value of FWHM. Lastly, the interaction effect of the experimental conditions, foot regions, and subtasks shows no statistical significance ($F = 0.13, P = 1.00, \eta^2 = 0.000$).

6. DISCUSSION

Given the potential of aBSE to increase the risk of its users directly or indirectly, this study empirically evaluates the implication of using aBSE for construction framing task using foot plantar pressure distribution data captured with wearable pressure insoles. In this section, the outcomes of the fall risk metrics are discussed and are peak pressure, average pressure, pressure-time integral, maximum pressure gradient and full width at half maximum.

6.1. Peak pressure

The results from the fall risk assessments demonstrate significant variations in peak pressure across different foot regions and subtasks when comparing the conditions with and without the use of an aBSE. The use of aBSE significantly increases the peak pressure of users in at least one foot region across all subtasks, indicating a higher risk of fall. Given that peak pressure represents the highest-pressure value at each foot region, the comparison between the two conditions (with-aBSE and without-aBSE) demonstrates an unsafe situation when using the aBSE. This is particularly significant in the heel and arch regions, which exhibit higher pressures across multiple subtasks, as shown in Fig. 5a-f. While the arch region's significance is somewhat surprising, the combination of heel and metatarsal pressure aligns with expectations given the postures assumed during subtasks (e.g., squatting, bending, and standing). The weight of the body is typically on either the metatarsal during squatting or the heel during standing and bending. This finding aligns with results from Mickle et al. [33], which also found significant peak pressure in the heel and metatarsal when comparing fallers and non-fallers. The moving subtask, which involves participants carrying a frame and moving across a staircase, exhibited the highest peak pressure. This is a reasonable result given the physical demands and dynamic nature of the task. Overall, the use of an exoskeleton substantially increases the risk of falls during construction framing work, particularly during dynamic and physically demanding tasks.

6.2. Average pressure

Although there were no significant differences in mean pressure across the four foot regions (i.e., heel, arch, metatarsal, and toe) during the measuring subtask, notable patterns emerged during other subtasks when using the aBSE. This finding is somewhat surprising given the squatting posture assumed during the measuring subtask, despite the additional weight of the device. It suggests that using the aBSE in a static position does not substantially increase fall risk.

The average pressure represents the mean pressure exerted by participants across all foot regions. It reveals that one or more foot regions consistently indicated fall risk across all subtasks except the measuring subtask. As shown in Fig. 6, the toe, metatarsal, and arch regions showed significant differences, suggesting no impact on the heel region whether using aBSE or not. Similarly, Antwi-Afari and Li [4] also identified these areas as significant in their study on different loss of balance events. For example, the notable increase in mean pressure in the toe region during the assembly subtask (14.2 % increase, $p = 0.04$) suggests that aBSE use may affect stability in this region, potentially impacting workers' balance during tasks requiring precision. Additionally, the increased mean pressure in the arch and metatarsal regions during the nailing subtask (19.4 % and 17.1 % increases, respectively, $p < 0.05$) could pose a

heightened risk of injury in these areas. This may lead to discomfort or fatigue over time, potentially compromising workers' safety and efficiency. During the lifting subtask, the significant increase in metatarsal pressure (27.6 % increase, $p = 0.00$) underscores the impact of aBSE on this foot region, potentially leading to instability or difficulties in lifting heavy objects. Similarly, the rise in arch pressure during the moving subtask (16 % increase, $p = 0.00$) highlights the importance of foot region support in tasks involving dynamic movements. Interaction effects between foot regions and subtasks, especially with the toe region showing the highest average pressure during assembly, nailing, lifting, and installation subtasks, suggest that these areas may need targeted ergonomic interventions and protective measures.

6.3. Pressure-Time integral

The pressure-time integral results illustrated in Fig. 7 demonstrate how the use of an aBSE influences fall risk across various subtasks and foot regions. The pressure-time integral represents the total pressure exerted by the participants over the period and the results show that moving subtask stands out as the only subtask with significant difference across all the foot regions. This indicates that the use of the aBSE brought significant changes in the participants' gait stability while moving the frame across the staircase, potentially increasing the risk of falls during more dynamic and intense framing tasks. These results align with peak pressure results and indicate that aBSE use may elevate fall risk in construction tasks involving significant movement. One significant finding is the increased pressure-time integral across the foot regions and subtasks when using the aBSE. For example, the toe region exhibited the highest pressure-time integral across all subtasks when using the aBSE, likely due to the nature of tasks such as squatting, bending, and other dynamic movements. This finding highlights the potential need for targeted interventions to support these critical areas during specific tasks. The interaction effect analysis also provided interesting insights. While there were no significant interactions between experimental conditions and foot regions or between experimental conditions and subtasks, there was a significant interaction between foot regions and subtasks. The highest pressure-time integral values were observed in the toe region during the assembly and measuring subtasks. This suggests that specific foot regions and tasks could benefit from particular attention to reduce fall risk.

Comparisons to previous studies, such as Choi et al. [13], revealed contrasts in the analysis of different loss of balance events and foot region pressures, further emphasizing the impact of specific tasks and equipment on fall risk. In particular, the repetitive body movements in measuring and assembly subtasks, combined with a higher pressure-time integral, indicate a greater risk of falling compared to other subtasks.

6.4. Maximum pressure gradient

The maximum pressure gradient represents the highest rate of change in the pressure across each of the foot regions and the results that there is at least a significant difference in the foot regions across the subtasks, except for moving. This indicates that the use of the aBSE substantially increases the risk of fall. While it was anticipated that the use of aBSE would affect the stability of the users while moving on a staircase with a 20 kg frame, surprisingly, the opposite is the case. The metatarsal foot region emerged as the most sensitive region to fall risk, as it is significant in three of the six subtasks. This result is in contrast with Yan et al. [55], where the arch and the heel were identified as the most sensitive regions for fall risk in elderly people during walking exercises. Such discrepancies highlight the importance of considering different populations and tasks when examining fall risk. Similar to the pressure-time integral, measuring and assembly subtasks represent the subtasks with the highest fall risk. This highlights the importance of identifying tasks that are particularly vulnerable to fall risks.

Understanding the tasks that are vulnerable to the risk of fall could help the safety managers to understand the crew the device would safely work for on the construction site.

6.5. Full width at half maximum (FWHM)

Although the main effects of the experimental conditions were not statistically significant, the paired *t*-test of the full width at half maximum (FWHM) for each foot region in different subtasks provided a deeper understanding of how aBSE usage could affect construction workers. The analysis of FWHM results reveals significant changes in all four foot regions during both measuring and moving subtasks. However, intriguingly, these two sets of results contradict each other: the moving subtask suggests that the use of aBSE increases fall risk, while the measuring subtask indicates the opposite. Although these conflicting results are not mirrored in other metrics, the outcomes of the moving subtask, which involves manually transporting frames to upper floors via staircases, align with other metrics and support the notion that the use of aBSE escalates fall risk during dynamic and demanding tasks. The statistical significance of the moving subtask results echoes findings by Yan et al. [55], who observed significant differences in FWHM across all foot regions when comparing the gait patterns of two elderly individuals during walking tasks. This suggests potential parallels in the effects of movement and balance across different populations and contexts. For the without-aBSE condition, measuring subtask showed significantly higher FWHM in all foot regions (heel, arch, metatarsal, and toe), indicating a potential risk for loss of balance events and subsequent falls. This finding highlights the importance of focusing on the measuring subtask in construction work, as workers may be more susceptible to injuries in this subtask due to uneven pressure distribution on their feet. These findings highlight the importance of investigating and monitoring the impact of aBSEs on construction tasks, particularly measuring and assembly, which had the highest FWHM values and pressure-related metrics. Consequently, there is a pressing need for more comprehensive research to elucidate the relationships among various foot plantar metrics.

6.6. Overall metrics

Overall, across all the metrics, the use of aBSE significantly increases the risk of falling in at least one of the subtasks. This may be attributed to the features of the aBSE and the nature of the construction work. While using the aBSE, the toe and the heel foot regions are the most sensitive regions according to all the metrics, except FWHM where metatarsal was revealed as the highest. With moving, measuring, and assembly being the most sensitive subtasks, this was not surprising because of the postures assumed including squatting and bending, which could isolate the pressure of the body in these foot regions. In response to the objective of this study, which is to evaluate fall risk while using aBSE in performing construction framing tasks, the results demonstrate that the use of aBSE could elevate fall risk, especially when the construction task is dynamic and demanding, as revealed by the results of all the computed metrics. Similar to Antwi-Afari et al. [3] and Yan et al. [55] where foot plantar pressure metrics have been employed to assess fall risk, this study demonstrates the efficacy of these metrics in assessing fall risk of using aBSE on construction sites.

7. Contributions

This study investigates the associated fall risk of using aBSE while performing construction framing tasks through the foot plantar pressure metrics of wearable pressure insoles. The study makes both theoretical and practical contributions in the following ways:

8. Theoretical contributions

This study makes several important theoretical contributions to construction safety research, particularly in the context of aBSEs and their impact on fall risk during construction work. By empirically evaluating foot plantar pressure distribution data, this study offers an understanding of how aBSE usage affects different foot regions and subtasks within construction framing work. These are described as follows: Firstly, the findings regarding peak pressure variations across different foot regions and subtasks with and without aBSEs provide insights into the complex relationship between foot pressure distribution and fall risk. The significant variations observed, particularly in the heel and metatarsal regions, suggest that aBSEs could lead to unsafe conditions and elevate fall risk during construction tasks. Secondly, the study contributes to the understanding of mean pressure differences across foot regions during different construction tasks. The data highlights how aBSE use may affect stability and risk of injury, particularly in dynamic and demanding tasks, such as nailing, lifting, and moving. Moreover, the analysis of pressure-time integral and maximum pressure gradient offers new perspectives on how aBSEs influence fall risk across different subtasks and foot regions. These metrics reveal the nuanced impact of aBSE use on gait stability and foot pressure distribution, particularly in dynamic tasks such as moving. Finally, the study of the full width at half maximum (FWHM) provides theoretical insights into how aBSE usage can either increase or decrease fall risk depending on the specific sub-task. This duality highlights the complex relationship between aBSEs and fall risk in construction work.

9. Practical contributions

The practical contributions of this study are centered around improving construction safety practices and interventions for workers using aBSEs. The results offer insights that can guide the development of ergonomic interventions and protective measures for workers performing construction tasks such as framing. The findings suggest that the toe and heel foot regions require special attention due to their sensitivity to increased pressure and fall risk when using aBSEs. Safety managers and ergonomists could use this information to implement interventions such as enhanced footwear support or training programs that focus on safe movements in these regions. Additionally, the identification of specific subtasks (e.g., measuring, moving, and assembly) that are particularly susceptible to fall risk provides guidance for safety protocols and aBSE usage. Workers and supervisors can benefit from this knowledge by adjusting work practices and using aBSEs more effectively during these tasks. Furthermore, the data on pressure-time integral and maximum pressure gradient highlights the need for ongoing monitoring and assessment of workers' safety while using aBSEs. Safety managers can use these metrics to identify potential hazards and implement preventative measures to reduce fall risk during dynamic and physically demanding tasks. Lastly, the study emphasizes the importance of continued research and data collection on aBSE use in construction, which can lead to better safety standards and improved working conditions for construction workers. By integrating foot plantar pressure metrics into safety assessments, construction sites can benefit from more effective approaches to fall risk management.

10. Conclusion, limitations, and future work

Given the biomechanical benefits attributed to the use of exoskeletons across various industry sectors, the construction industry is preparing for the adoption of aBSE to reduce the threat of WMSDs. Noticeably, there have been unintended consequences that could directly or indirectly raise fall hazard issues while using exoskeletons on construction sites. This study evaluates the fall risk implications of using aBSE for carpentry framing task. The results show that the use of aBSE significantly increased the foot pressure metrics in at least one of the

subtasks and foot regions, with an increase ranging from 7 % to 51 %. This suggests an elevated fall risk associated with using the device. Across all the metrics, the toe and heel regions showed the highest increases, indicating they are most sensitive to changes in gait. The moving, measuring, and assembly subtasks were found to carry the highest risk of falling, as evidenced by their high pressure values.

While this study shows that there is a risk of falling, there are some inconsistencies in results of the metrics used. Further study should examine the relationship between these metrics in the context of construction-related tasks to identify the most important metrics. Conducting studies in real-world construction settings and with a larger sample would provide more generalizable results, as this study was conducted in a controlled laboratory environment simulating carpentry tasks. Moreover, including a more diverse sample of experienced construction workers in future studies could lead to more comprehensive insights. Future studies could explore participants' subjective evaluations of fall risk while using aBSEs. This study provides insights into the potential risks of falling while using aBSEs in construction and informs stakeholders about the need for careful decision-making regarding their adoption. The results contribute to the understanding of the relationship between foot regions, fall risk metrics, and construction tasks, and inform how aBSEs could be designed to better suit construction work.

CRediT authorship contribution statement

Akinwale Okunola: Writing – review & editing, Writing – original draft, Visualization, Software, Project administration, Methodology, Investigation, Formal analysis, Conceptualization. **Abiola Akanmu:** Writing – review & editing, Writing – original draft, Project administration, Methodology, Investigation, Funding acquisition, Formal analysis, Conceptualization. **Houtan Jebelli:** Writing – review & editing, Supervision, Project administration, Methodology, Funding acquisition, Conceptualization.

Declaration of competing interest

The authors declare that they have no known competing financial interests or personal relationships that could have appeared to influence the work reported in this paper.

Data availability

Data will be made available on request.

Acknowledgment

This material is based upon work supported by the National Science Foundation under Grant Nos. 2221166 and 2221167. Any opinions, findings, conclusions, or recommendations expressed in this material are those of the author(s) and do not necessarily reflect the views of the National Science Foundation.

References

- [1] K. Anam, A.A. Al-Jumaily, Active exoskeleton control systems: State of the art, *Procedia Eng.* 41 (2012) 988–994, <https://doi.org/10.1016/j.proeng.2012.07.273>.
- [2] V.F. Annese, D. De Venuto, "FPGA based architecture for fall-risk assessment during gait monitoring by synchronous EEG/EMG." *Proc.*, 2015 6th International Workshop on Advances in Sensors and Interfaces (IWASI), IEEE, 116–121.
- [3] M.F. Antwi-Afari, S. Anwer, W. Umer, H.-Y. Mi, Y. Yu, S. Moon, M.U. Hossain, Machine learning-based identification and classification of physical fatigue levels: A novel method based on a wearable insole device, *Int. J. Ind. Ergon.* 93 (2023) 103404, <https://doi.org/10.1016/j.ergon.2022.103404>.
- [4] M.F. Antwi-Afari, H. Li, Fall risk assessment of construction workers based on biomechanical gait stability parameters using wearable insole pressure system, *Adv. Eng. Inf.* 38 (2018) 683–694, <https://doi.org/10.1016/j.aei.2018.10.002>.
- [5] S. Anwer, H. Li, M.F. Antwi-Afari, A.M. Mirza, M.A. Rahman, I. Mehmood, R. Guo, A.Y.L. Wong, Evaluation of Data Processing and Artifact Removal Approaches Used for Physiological Signals Captured Using Wearable Sensing Devices during Construction Tasks, *J. Constr. Eng. Manag.* 150 (1) (2024) 03123008, <https://doi.org/10.1061/JCEMD4.COENG-13263>.
- [6] P. Bet, P.C. Castro, M.A. Ponti, Fall detection and fall risk assessment in older person using wearable sensors: A systematic review, *Int. J. Med. Inf.* 130 (2019) 103946, <https://doi.org/10.1016/j.ijmedinf.2019.08.006>.
- [7] T. Bosch, J. van Eck, K. Knitel, M. de Looze, The effects of a passive exoskeleton on muscle activity, discomfort and endurance time in forward bending work, *Appl. Ergon.* 54 (2016) 212–217, <https://doi.org/10.1016/j.apergo.2015.12.003>.
- [8] P.E. Caicedo, C.F. Rengifo, L.E. Rodriguez, W.A. Sierra, M.C. Gómez, Dataset for gait analysis and assessment of fall risk for older adults, *Data Brief* 33 (2020) 106550, <https://doi.org/10.1016/j.dib.2020.106550>.
- [9] C. Chatzaki, V. Skaramagkas, N. Tachos, G. Christodoulakis, E. Maniadi, Z. Kefalopoulou, D.I. Fotiadis, M. Tsiknakis, The smart-insole dataset: Gait analysis using wearable sensors with a focus on elderly and Parkinson's patients, *Sensors* 21 (8) (2021) 2821, <https://doi.org/10.3390/s21082821>.
- [10] M. Chen, H. Wang, L. Yu, E.H.K. Yeung, J. Luo, K.-L. Tsui, Y. Zhao, A systematic review of wearable sensor-based technologies for fall risk assessment in older adults, *Sensors* 22 (18) (2022) 6752, <https://doi.org/10.3390/s22186752>.
- [11] S. Choi, H. Cho, B. Kang, D.H. Lee, M.J. Kim, S.H. Jang, Slip-related changes in plantar pressure distribution, and parameters for early detection of slip events, *Ann. Rehabil. Med.* 39 (6) (2015) 897–904, <https://doi.org/10.5535/arm.2015.39.6.897>.
- [12] R.N. Ferreira, N.F. Ribeiro, C.P. Santos, Fall risk assessment using wearable sensors: a narrative review, *Sensors* 22 (3) (2022) 984, <https://doi.org/10.3390/s22030984>.
- [13] S. Fox, O. Aranko, J. Heilala, P. Vahala, Exoskeletons: Comprehensive, comparative and critical analyses of their potential to improve manufacturing performance, *J. Manuf. Technol.* 31 (6) (2019) 1261–1280, <https://doi.org/10.1108/JMT-01-2019-0023>.
- [14] German-Bionic (2023). "CrayX." <https://germanbionic.com/en/solutions/exo_skeletons/crayx/>. (September, 8, 2023).
- [15] N.J. Gonsalves, O.O. Ogunseju, A.A. Akanmu, C.A. Nnaji, Assessment of a passive wearable robot for reducing low back disorders during rebar work, *J. Inf. Technol. Constr.* 26 (2021) (2021) 936–952, <https://doi.org/10.36680/j.itcon.2021.050>.
- [16] R. Govaerts, S. De Bock, S. Provyn, B. Vanderborght, B. Roelands, R. Meeusen, K. De Pauw, The impact of an active and passive industrial back exoskeleton on functional performance, *Ergonomics* 67 (5) (2024) 597–618, <https://doi.org/10.1080/00140139.2023.2236817>.
- [17] K. Huysamen, M. de Looze, T. Bosch, J. Ortiz, S. Toxiri, L.W. O'Sullivan, Assessment of an active industrial exoskeleton to aid dynamic lifting and lowering manual handling tasks, *Appl. Ergon.* 68 (2018) 125–131, <https://doi.org/10.1016/j.apergo.2017.11.004>.
- [18] M. Jeong, H. Woo, K. Kong, A study on weight support and balance control method for assisting squat movement with a wearable robot, angel-suit, *Int. J. Control. Autom. Syst.* 18 (2020) 114–123, <https://doi.org/10.1007/s12555-019-0243-x>.
- [19] K. Khalaf, D.M. Mohan, M. Al Hindi, A.H. Khandoker, H.F. Jelinek, Plantar pressure alterations associated with increased BMI in young adults, *Gait Posture* 98 (2022) 255–260, <https://doi.org/10.1016/j.gaitpost.2022.09.071>.
- [20] J. Kim, K. Kim, C. Gubler, Comparisons of plantar pressure distributions between the dominant and non-dominant sides of older women during walking, *J. Phys. Ther. Sci.* 25 (3) (2013) 313–315, <https://doi.org/10.1589/jpts.25.313>.
- [21] S. Kim, A. Moore, D. Srinivasan, A. Akanmu, A. Barr, C. Harris-Adamson, D. M. Rempel, M.A. Nussbaum, Potential of exoskeleton technologies to enhance safety, health, and performance in construction: Industry perspectives and future research directions, *IIEE Transactions on Occupational Ergonomics and Human Factors* 7 (3–4) (2019) 185–191, <https://doi.org/10.1080/24725838.2018.1561557>.
- [22] C.-H. Lee, T.-L. Sun, Evaluation of postural stability based on a force plate and inertial sensor during static balance measurements, *J. Physiol. Anthropol.* 37 (2018) 1–16, <https://doi.org/10.1186/s40101-018-0187-5>.
- [23] A. Leone, G. Rescio, P. Siciliano, "Fall risk evaluation by surface electromyography technology." *Proc.*, 2017 International Conference on Engineering, Technology and Innovation (ICE/ITMC), IEEE, 1092–1095. Doi: 10.1109/ICE.2017.8280003.
- [24] J. Liu, X. Zhang, T.E. Lockhart, Fall risk assessments based on postural and dynamic stability using inertial measurement unit, *Saf. Health Work* 3 (3) (2012) 192–198, <https://doi.org/10.5491/SHAW.2012.3.3.192>.
- [25] Y. Liu, X. Li, J. Lai, A. Zhu, X. Zhang, Z. Zheng, H. Zhu, Y. Shi, L. Wang, Z. Chen, The effects of a passive exoskeleton on human thermal responses in temperate and cold environments, *Int. J. Environ. Res. Public Health* 18 (8) (2021) 3889, <https://doi.org/10.3390/ijerph18083889>.
- [26] C. Marchand, J.B. De Graaf, N. Jarrassé, Measuring mental workload in assistive wearable devices: a review, *Journal of NeuroEngineering and Rehabilitation* 18 (1) (2021) 1–15, <https://doi.org/10.1186/s12984-021-00953-w>.
- [27] A. Mehmood, A. Nadeem, M. Ashraf, M.S. Siddiqui, K. Rizwan, K. Ahsan, A fall risk assessment mechanism for elderly people through muscle fatigue analysis on data from body area sensor network, *IEEE Sens. J.* 21 (5) (2020) 6679–6690, <https://doi.org/10.1109/JSEN.2020.3043285>.
- [28] H.B. Menz, G.V. Zammit, S.E. Munteanu, Plantar pressures are higher under calloused regions of the foot in older people, *Clin. Exp. Dermatol.* 32 (4) (2007) 375–380, <https://doi.org/10.1111/j.1365-2230.2007.02421.x>.
- [29] K.J. Mickle, B.J. Munro, S.R. Lord, H.B. Menz, J.R. Steele, Foot pain, plantar pressures, and falls in older people: a prospective study, *J. Am. Geriatr. Soc.* 58 (10) (2010) 1936–1940, <https://doi.org/10.1111/j.1532-5415.2010.03061.x>.
- [30] Moticon-OpenGO (2023). "OpenGo sensor insoles." <<https://moticon.com/opengo/sensor-insoles>>. (12/03/2023, 2023).

- [35] S.G.R. Neri, A.B. Gadelha, A.L.M. Correia, J.C. Pereira, A.C. de David, R.M. Lima, Obesity is associated with altered plantar pressure distribution in older women, *J. Appl. Biomech.* 33 (5) (2017) 323–329, <https://doi.org/10.1123/jab.2016-0357>.
- [36] O. Ogunseiju, J. Olayiwola, A. Akanmu, O.A. Olatunji, Evaluation of postural-assist exoskeleton for manual material handling, *Eng. Constr. Archit. Manag.* 29 (3) (2022) 1358–1375, <https://doi.org/10.1108/ECAM-07-2020-0491>.
- [37] O.R. Ogunseiju, J. Olayiwola, A.A. Akanmu, C. Nnaji, Digital twin-driven framework for improving self-management of ergonomic risks, *Smart and Sustainable Built Environment* 10 (3) (2021) 403–419, <https://doi.org/10.1108/SASBE-03-2021-0035>.
- [38] A. Okunola, A.A. Akanmu, A.O. Yusuf, Comparison of active and passive back-support exoskeletons for construction work: range of motion, discomfort, usability, exertion and cognitive load assessments, ahead-of-print(ahead-of-print). Doi: Smart and Sustainable Built Environment (2023) <https://doi.org/ezproxy.lib.vt.edu/10.1108/SASBE-06-2023-0147>.
- [39] J.-H. Park, S. Kim, M.A. Nussbaum, D. Srinivasan, Effects of two passive back-support exoskeletons on postural balance during quiet stance and functional limits of stability, *J. Electromyogr. Kinesiol.* 57 (2021) 102516, <https://doi.org/10.1016/j.jelekin.2021.102516>.
- [40] J. Park, Assessing the Effects of Exoskeleton Use on Balance and Postural Stability, Virginia Tech. (2021). <https://vtechworks.lib.vt.edu/items/bceab73a-ad93-4705-bfc1-7f41a7560568>.
- [41] M.T. Picchiotti, E.B. Weston, G.G. Knapik, J.S. Dufour, W.S. Marras, Impact of two postural assist exoskeletons on biomechanical loading of the lumbar spine, *Appl Ergon* 75 (2019) 1–7, <https://doi.org/10.1016/j.apergo.2018.09.006>.
- [42] T. Poliero, V. Fanti, M. Sposito, D.G. Caldwell, C. Di Natali, Active and passive back-support exoskeletons: a comparison in static and dynamic tasks, *IEEE Rob. Autom. Lett.* 7 (3) (2022) 8463–8470, <https://doi.org/10.1109/LRA.2022.3188439>.
- [43] T. Poliero, M. Lazzaroni, S. Toxiri, C. Di Natali, D.G. Caldwell, J. Ortiz, Applicability of an active back-support exoskeleton to carrying activities, *Front Robot Ai* 7 (2020) 579963, <https://doi.org/10.3389/frobt.2020.579963>.
- [44] F.T. Price, Validation of a wearable sensor insole device for analysis of postural control, Miami University. (2018). https://etd.ohiolink.edu/acprod/odb_etd/ws/send_file/send?accession=miami152517168199145&disposition=inline.
- [45] S. Raghu, N. Sriram, E.D. Gommer, D.M. Hilkman, Y. Temel, S.V. Rao, P. L. Kubben, Adaptive median feature baseline correction for improving recognition of epileptic seizures in ICU EEG, *Neurocomputing* 407 (2020) 385–398, <https://doi.org/10.1016/j.neucom.2020.04.144>.
- [46] R. Shah, The NIOSH lifting equation for manual lifting and its applications, *Journal of Ergonomics* 6 (2) (2016) 1–10, <https://doi.org/10.4172/2165-7556.1000159>.
- [47] Z. Song, J. Ou, L. Shu, G. Hu, S. Wu, X. Xu, Z. Chen, Fall risk assessment for the elderly based on weak foot features of wearable plantar pressure, *IEEE Trans. Neural Syst. Rehabil. Eng.* 30 (2022) 1060–1070, <https://doi.org/10.1109/TNSRE.2022.3167473>.
- [48] S. Subramaniam, A.I. Faisal, M.J. Deen, Wearable sensor systems for fall risk assessment: A review, *Frontiers in Digital Health* 4 (2022) 921506, <https://doi.org/10.3389/fdgth.2022.921506>.
- [49] A. Tandle, N. Jog, P. D'cunha, M. Chhetra, Classification of artefacts in EEG signal recordings and overview of removing techniques, *International Journal of Computer Applications* 975 (2015) 8887.
- [50] B.M. Tehrani, J. Wang, D. Truax, Assessment of mental fatigue using electroencephalography (EEG) and virtual reality (VR) for construction fall hazard prevention, *Eng. Constr. Archit. Manag.* 29 (9) (2022) 3593–3616, <https://citeseerx.ist.psu.edu/document?repid=rep1&type=pdf&doi=cba7b93c6810a7bbc5917bbafe419fdc6fb6396>.
- [51] S. Toxiri, M.B. Naf, M. Lazzaroni, J. Fernández, M. Sposito, T. Poliero, L. Monica, S. Anastasi, D.G. Caldwell, J. Ortiz, Back-support exoskeletons for occupational use: an overview of technological advances and trends, *IIE Transactions on Occupational Ergonomics and Human Factors* 7 (3–4) (2019) 237–249, <https://doi.org/10.1080/24725838.2019.1626303>.
- [52] S. Upasani, R. Franco, K. Niewolny, D. Srinivasan, The potential for exoskeletons to improve health and safety in agriculture—Perspectives from service providers, *IIE Transactions on Occupational Ergonomics and Human Factors* 7 (3–4) (2019) 222–229, <https://doi.org/10.1080/24725838.2019.1575930>.
- [53] T. Walter, N. Stützig, T. Siebert, Active exoskeleton reduces erector spinae muscle activity during lifting, *Front. Bioeng. Biotechnol.* 11 (2023) 1143926.
- [54] T.R. Waters, V. Putz-Anderson, A. Garg, 1994. “Applications manual for the revised NIOSH lifting equation.” Doi: 10.3389/fbioe.2023.1143926.
- [55] Y. Yan, J. Ou, H. Shi, C. Sun, L. Shen, Z. Song, L. Shu, Z. Chen, Plantar pressure and falling risk in older individuals: a cross-sectional study, *Journal of Foot and Ankle Research* 16 (1) (2023) 1–11, <https://doi.org/10.1186/s13047-023-00612-4>.
- [56] A. Yıldız, Towards Environment-Aware Fall Risk Assessment: Classifying Walking Surface Conditions Using IMU-Based Gait Data and Deep Learning, *Brain Sci.* 13 (10) (2023) 1428, <https://doi.org/10.3390/brainsci13101428>.
- [57] Z. Zhou, Y.M. Goh, Q. Shi, H. Qi, S. Liu, Data-driven determination of collapse accident patterns for the mitigation of safety risks at metro construction sites, *Tunn. Undergr. Space Technol.* 127 (2022) 104616, <https://doi.org/10.1016/j.tust.2022.104616>.
- [58] Y. Zhu, C. Johnson, S.-H.J. Chang, R.K. Mehta, “Neuroergonomics metrics to evaluate Exoskeleton based Gait Rehabilitation.” Proc., 2020 IEEE International Conference on Systems, Man, and Cybernetics (SMC), IEEE, 3447-3453. Doi: 10.1109/SMC42975.2020.9283238.